The influence of disorder on the optical properties of III-N-based resonant Bragg structures

© A.A. Ivanov[1], V.V. Chaldyshev[1], E.E. Zavarin[1], A.V. Sakharov[1], V.V. Lundin[1], A.F. Tsatsulnikov[2]

[1] Ioffe Institute,
194021 St. Petersburg, Russia
[2] Submicron Heterostructures for Microelectronics Research and Engineering Center of the Russian Academy of Sciences,
194021 St. Petersburg, Russia

E-mail: aleksei98.ivanov@mail.ioffe.ru

Received December 5, 2024
Revised December 6, 2024
Accepted December 6, 2024

The effect of spatial and energy disorder on the formation of a superradiant exciton-polariton mode in the reflectance spectra of resonant Bragg structures (RBSs) at room temperature is studied. A limitation on the number of InGaN quantum wells (QWs) in RBS caused by critical spatial disorder is found. This disorder determines the transformation of a single superradiant optical mode into a multimode spectrum. A record high exciton oscillator strength in GaN QW compared to other material systems is experimentally achieved. The increase in the exciton oscillator strength in GaN QW compared to InGaN QW is mainly explained by a decrease in the inhomogeneous broadening of the exciton state.

Keywords: Resonant Bragg structures, quantum wells, excitons, exciton resonance, Bragg resonance, gallium nitride.

DOI: 10.61011/SC.2024.11.59953.05S

1. Introduction

Enhancing the interaction between light and matter is a major challenge faced by modern nanophotonics [1,2]. Efficient coupling between electromagnetic waves and quasi-dimensional excitons can be achieved by using a microresonator [3] or by creating an optical lattice of multiple semiconductor quantum wells (QWs) distributed in space [4]. The latter approach is realised in the so-called resonant Bragg structures (RBS), which were first theoretically proposed in [5]. In RBS, the period of the structure is chosen so that the Bragg diffraction condition is fulfilled at the wavelength of excitons in the QWs. In an ideal RBS composed of N QWs, a single mode is optically active, which is called the superradiative exciton-polariton mode [6]. The oscillator strength and radiative decay of this mode turns out to be N times greater compared to a single QW. The light reflection coefficient from the RBS of N QW without taking into account the dielectric contrast between the QW material and the barrier is determined by the following expression [5]:

$$R_N(\omega) = \frac{(N\Gamma_0)^2}{(\omega_0 - \omega)^2 + (\Gamma + N\Gamma_0)^2}, \qquad (1)$$

where Γ and Γ_0 — non-radiative and radiative exciton decay in the QW, respectively, N — the number of QWs, ω_0 — the resonant frequency of the exciton in the QW, ω — the frequency of the incident light wave. Usually, for a single QW, the nonradiative losses are quite high $\Gamma > \Gamma_0$. However, the collective interaction of quasi-dimensional excitons with light in RBS with a sufficiently large number of QWs can provide $N\Gamma_0 > \Gamma$, i.e., radiating processes can become more effective than non-radiating ones.

So far, the formation of a superradiant mode in RBS has been experimentally confirmed for various material systems. RBS based on (Cd,Mn)Te/(Cd,Zn,Mg)Te [7–9], In(As,P)/InP [10], (In,Ga)As/GaAs [11–15], InAs/GaAs [16,17], and GaAs/(Al,Ga)As [18–23] showed efficient interaction of light with excitons in QWs at cryogenic temperatures. However, the exciton binding energy in such QWs turns out to be insufficient for RBS operation at room temperature.

High binding energy and oscillator strength of excitons in III-N-based QWs allow us to observe a resonant exciton response from RBS at temperatures up to room temperature. The development of modern epitaxial technology of GaN family materials allowed us to demonstrate the formation of a superradiant mode at room temperature in RBS from (In,Ga)N/GaN [24–33] and GaN/(Al,Ga)N [34] QWs.

The concept of an ideal RBS assumes a strict periodicity of the QWs and the identity of exciton states in them. Unfortunately, in real systems there is always some disorder, because the thickness and composition of the layers can be controlled with a certain accuracy. In addition, if the material of the QW and (or) barrier is a multicomponent semiconductor alloy, the exciton states depend on spatial fluctuations of the alloy composition [35]. This leads to inhomogeneous broadening of exciton states in the QW. Obviously, these effects negatively affect the optical and electro-optical properties of RBS.

It is especially relevant to analyse the influence of the disorder in heterostructures based on III-N, since these materials are used for the creation and mass production of

various modern optoelectronic devices [36,37]. Thus, random fluctuations of indium concentration in the (In,Ga)N alloy have been widely discussed over the last decade because they lead to carrier localisation effects [38–44], the appearance of Urbach tails [45,46] and a decrease in the mobility of the two-dimensional electron gas [47]. All these phenomena lead to a decrease in the efficiency of (In,Ga)N/GaN LEDs [48–50]. Thus, the effect of disorder on the optical and electronic properties in III-N-based QWs is of interest not only from the fundamental but also from the practical point of view.

In this paper, we present the results of the influence of spatial and energetic disorder on the optical properties of RBS based on III-N. Using an experimentally verified model, we have found limitations on the creation of RBS with a large number of QWs caused by spatial disorder. We also experimentally obtained a record value of Γ_0 radiative decay in GaN QWs compared to (In,Ga)N QWs, which is explained by the reduction of inhomogeneous broadening of the exciton state.

2. Samples, experimental and calculation methods

Samples were grown by metalorganic chemical vapour deposition (MOCVD) using standard precursors — trimethyl gallium, triethyl gallium, trimethylaluminium, trimethylindium, and ammonia. In the case of InGaN structures, growth was carried out on GaN buffer layers grown on a sapphire (0001) substrate. When growing AlGaN-based structures, GaN buffer layers cannot be used due to light absorption in them, and growth was performed directly on sapphire substrates using a two-dimensional nucleation layer technique followed by growth of a wide-gap buffer transparent to GaN/(Al,Ga)N QW radiation. The same conditions were used for growing each barrier or QW in RBSs. The growth is described in more detail in [27,29]. The growth of nitride structures on sapphire substrates has a number of peculiarities related to differences in lattice constants and temperature coefficients of expansion. The use of nucleation layers allows removing most of the mismatch in the lattice parameter, but the growth of thick layers still accumulates elastic stresses causing the growing structure to bend. Since the optimal conditions for the growth of (In,Ga)N and GaN differ significantly, in particular in temperature, a change in temperature leads to a significant change in bending. In its turn, the bending of the substrate strongly affects the surface temperature and the indium [51] incorporation. Therefore, usually growth conditions are selected so that (In,Ga)N QWs are grown at near-zero surface curvature (Figure 1). However, such growth conditions lead to significant values of surface curvature during GaN growth, which also change during growth. In addition, during MOCVD, deposits may be deposited on the reactor surfaces, which leads to a decrease in the surface temperature of the growing layer at a constant

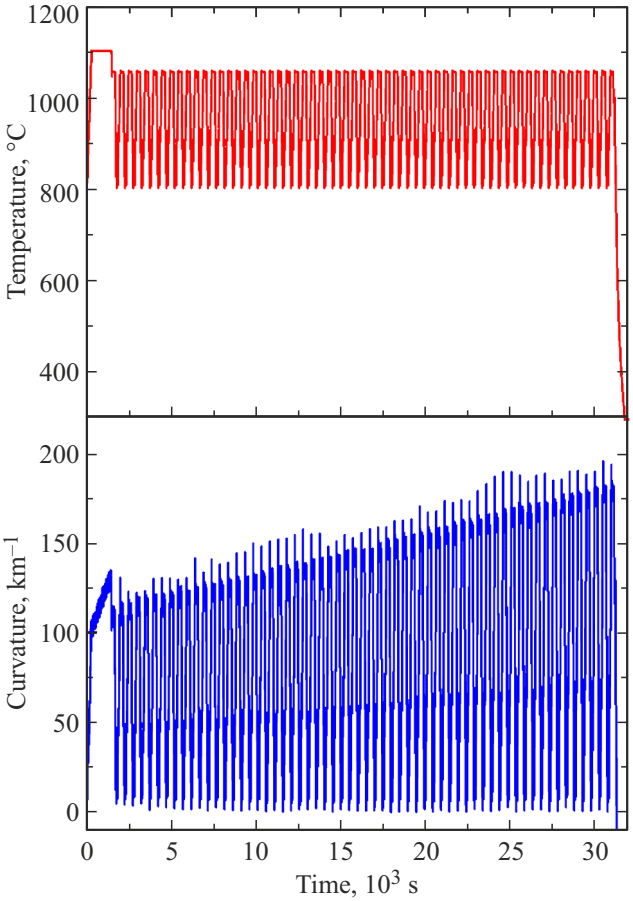

Figure 1. Variation of substrate holder temperature (red line) and heterostructure surface curvature (blue line) during the growth of a structure containing 100 (In,Ga)N/GaN QWs.

temperature of the substrate holder. The growth rate of GaN increases as the surface temperature decreases [52], this change is not so significant, 0.1–0.2%/°C, and in most device structures this change can be neglected. However, in a situation where it is necessary to grow very thick structures with maximum thickness control in each layer, it can cause problems. The features described above are much less pronounced for GaN/(Al,Ga)N structures, since growth is carried out at a constant substrate holder temperature, although the problem of changing the substrate curvature as the layer thickness increases persists in this case.

Reflectance spectra from the investigated samples were recorded at different light incidence angles. All measurements were performed for *s*- and *p*-polarisations of light at room temperature. The light source was a lamp made by „Hamamatsu Photonics K.K.“ model L6565, the light from which was passed through a polariser. A Glan–Taylor prism was used as the polariser. A quartz glass lens was used to focus the light into a small spot on the sample. The spectral characteristics were recorded using an Ocean Optics „solarisation resistant“ optical fibre and an Ocean Optics HR4000CG-UV-NIR spectrometer.

Numerical simulation of the optical properties of RBSs was fulfilled using the transfer matrix method. In this approach, each layer of the entire epitaxial system is described by a transfer matrix that relates the amplitudes of incoming and outgoing electromagnetic waves. The transfer matrices across the interfaces of the heterostructure are defined by Fresnel formulas. The transfer matrices through layers with quasi-dimensional excitons were formed based on the amplitude reflection and transmission coefficients for an exciton in a single QW [5]. A more detailed description of this calculation technique can be found in [29,31].

3. Spatial disorder

Figure 2 shows experimental and calculated spectra of resonant optical reflection from RBSs of 30 (Figure 2, *a*), 60 (Figure 2, *b*) and 100 (Figure 2, *c*) QW (In,Ga)N/GaN. The incidence angles of *p*-polarised light are chosen so that the exciton and Bragg resonance conditions are simultaneously fulfilled. We do not use anti-reflection coatings, so all spectra show background reflection depending on the angle of incidence according to the Fresnel formulas. Fabry-Perot oscillations due to reflections at the air/GaN and GaN/sapphire interfaces are also observed in the spectra. These oscillations gradually decay in the short-wavelength region of the reflectance spectra due to absorption in the QW (In,Ga)N and GaN barriers. Below the fundamental absorption edge of GaN (< 363 nm), the Fabry-Perot oscillations completely disappear.

In Figure 2, together with the experimental reflectance spectra (solid black lines), the calculated reflectance spectra taking into account exciton effects in the (In,Ga)N/GaN (dashed red lines) are presented. The calculated curves are in fairly good agreement with the experimental reflectance spectra, showing all important spectral features. The exciton parameters in the calculations are as follows: the exciton resonance energy $\hbar\omega_0 = 3.24$ eV for RBS out of 30 and 60 QW (In,Ga)N and $\hbar\omega_0 = 3.15$ eV for RBS out of 100 QW (In,Ga)N; the radiative decay parameter $\hbar\Gamma_0 = 0.22 \pm 0.02$ meV and the non-radiative decay parameter $\hbar\Gamma = 40 \pm 5$ meV for all the studied RBSs.

Figure 2 also shows the results of calculations without taking into account the exciton contribution to the reflectance spectra (i. e. $\Gamma_0 = 0$) with all other parameters remaining the same for all structures. From the comparison of the reflectance spectra with (dashed red lines) and without (dotted blue lines) the exciton effects, we conclude that the optical lattice of quasi-dimensional excitons makes a significant contribution to the resonant optical response of RBSs with QW (In,Ga)N/GaN.

The resonant optical reflection from 30 QW (In,Ga)N/GaN RBS is rather weak (Figure 2, *a*) because the non-radiative width of the exciton resonance Γ is much larger than the radiative width of 30 Γ_0 at room temperature. A significant enhancement of resonant optical reflection at room temperature is experimentally observed

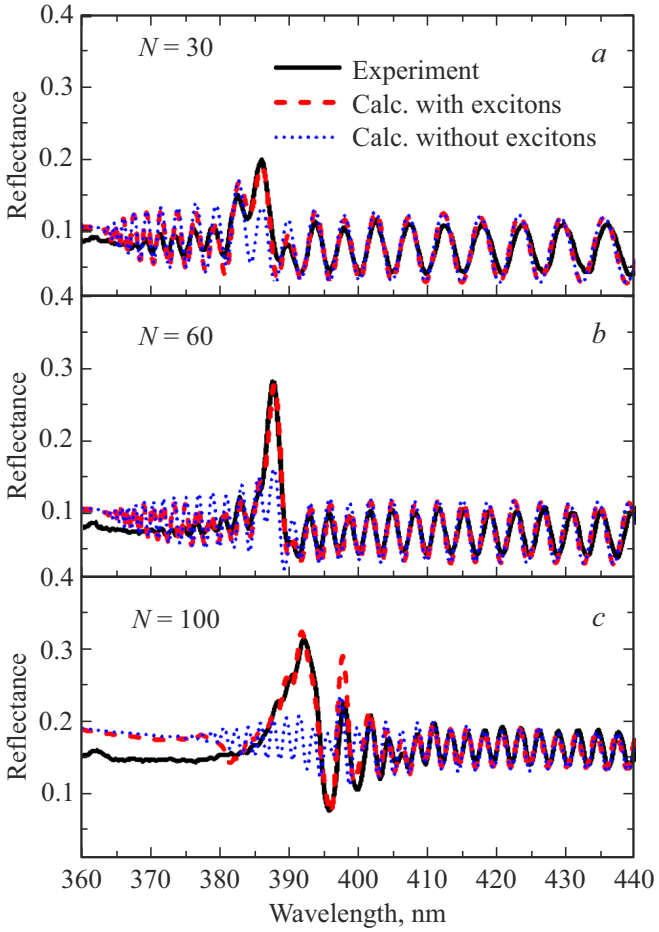

Figure 2. Experimental (solid black lines), calculated with excitons in QWs (dashed red lines), and calculated without the exciton contribution (dotted blue lines) spectra of resonant optical reflection from RBSs from 30 (*a*), 60 (*b*), and 100 (*c*) QWs (In,Ga)N/GaN. The light incidence angles are 20° for the RBSs of 30 (*a*), 60 (*b*), and 100 (*c*) QWs (In,Ga)N/GaN, respectively. Room temperature, *p*-polarisation of light. (A color version of the figure is provided in the online version of the paper).

in 60 QW (In,Ga)N/GaN RBS (Figure 2, *b*). According to equation (1), further increase in the number of QWs in the N RBS should lead to an even greater enhancement of the resonant optical characteristics.

Several spectrally separated reflection maxima are observed in the resonant optical reflection spectrum of 100 QW (In,Ga)N/GaN RBS (Figure 2, *c*). At the same time, the maximum reflection coefficient above the background level for 100 QW (In,Ga)N/GaN RBS is found to be the same as that for 60 QW (In,Ga)N/GaN RBS (Figure 2, *b*). In order to describe the observed diffraction pattern in the reflectance spectrum in Figure 2, *c*, the RBS of 100 QWs was defined by ten structural sets of 10 consecutive strictly periodic QWs in the calculation. The thickness of the (In,Ga)N layer in the whole RBS does not change and is 2.5 nm. Quantitatively, the spatial disorder in RBS can be described by the normalised standard

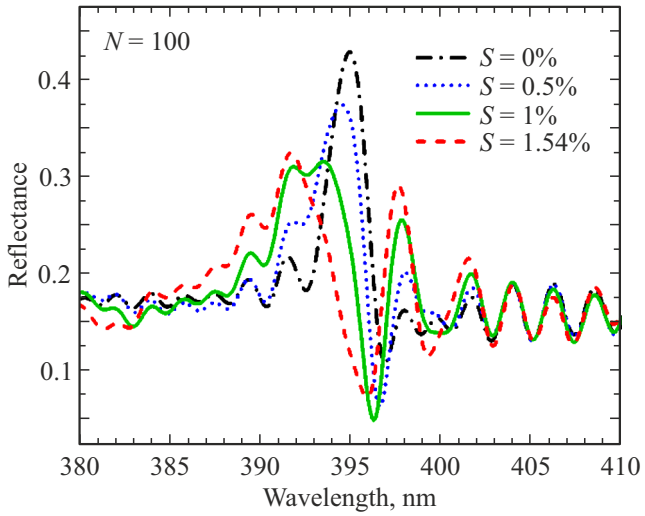

Figure 3. Calculated resonant optical reflectance spectra of 100 QW (In,Ga)N/GaN RBS with different value of standard deviation S. Light incidence angle 20°, room temperature, p-light polarisation.

deviation S:

$$S = \frac{1}{d}\sqrt{\frac{1}{n}\sum_{i=1}^{n}(d_i - \bar{d})^2}, \qquad (2)$$

where d_i — thickness of the i-th layer, $\bar{d}$ — the arithmetic mean layer thickness, n — the number of layers in the structure. For the calculated reflection spectra shown in Figure 2, c, the parameter S is 1.54%. Note that the experimentally observed enhancement of light reflection from 30 and 60 QW (In,Ga)N/GaN RBS (Figure 2, a and b) can be described within the framework of the strictly equidistant model ($S = 0$).

Figure 3 shows the spectra of resonant optical reflection from 100 QW (In,Ga)N/GaN RBS with different value of normalised standard deviation S. All spectra are calculated for p-polarised light incident at an angle 20° at room temperature. The set sequence and the magnitude of $(d_I - \bar{d})/(d_j - \bar{d})$ in the calculations remain constant for any pair i and j.

It can be seen from Figure 3 that the maximum optical reflection coefficient is observed for a strictly equidistant 100 RBS of (In,GaN)/GaN ($S = 0\%$). With increasing spatial disorder in the RBS, the resonance peak of light reflection from the RBS decreases insignificantly in amplitude and increases in width. n addition, the reflection peak shifts to the region of short wavelengths ($S = 0.5\%$). This shift is explained by a preferential decrease in the barrier thicknesses of the first 10 QW structural sets. Overall, the resonance spectrum of the RBS reflection is found to be quite robust to this small disorder $\sim 0.5\%$.

The resonant optical reflectance spectrum from the RBS undergoes a significant transformation when the spatial disorder is $\sim 1\%$. Now, instead of a single reflection peak, two weaker peaks spectrally separated from each other are observed. Such spatial disorder for the RBS turns out to be critical because it leads to the transformation of a single super-emitting mode into a multi-mode spectrum [32]. Further increase of spatial disorder in RBS leads to an increase in the number of reflection modes distributed over the spectrum. Since the spectral density of modes is proportional to the number of oscillators in a finite RBS, the critical disorder determined by the transition to the multimode regime is inversely proportional to the number of QWs in the RBS. This leads to the fact that an RBS composed of a large number of QWs is significantly more sensitive to the spatial disorder [32]. This result is confirmed by the experimental data shown in Figure 2. The presence of spatial disorder turns out to be critically important for RBS made of 100 QW (In,Ga)N/GaN, while for RBS made of 30 and 60 QW (In,Ga)N/GaN it turns out to be insignificant.

It should also be noted that the increased sensitivity of RBS with a large number of QWs to spatial disorder is not exclusive to the material system used in our study. In [15], it was determined that for strong resonant optical reflection from RBS of record 210 QW (In,Ga)As/GaAs, an error in the cell sequence periodicity should be less than one or two monolayers. It can be concluded that the enhancement of resonant optical properties of RBS, determined by the value of $N\Gamma_0$, by an unlimited increase in the number of QWs turns out to be impossible.

4. Energetic disorder

Exciton states in (In,Ga)N QWs have significant inhomogeneous broadening, which is caused by fluctuations in the width and chemical composition of the [53] QWs. These phenomena should be significantly reduced in GaN QWs with (Al,Ga)N barriers, since in this case the QW material is a binary compound. However, there will be some inhomogeneous broadening of exciton states of GaN QWs due to penetration of wave functions of electrons and holes into (Al,Ga)N barriers. The investigated QWs (In,Ga)N/GaN and GaN/(Al,Ga)N QWs have sufficient depth to ensure a high degree of wave function localisation inside the QWs, so the compositional disorder inside the QWs leads to a significantly larger inhomogeneous width of the exciton state in the QWs compared to the disorder in the barriers.

Figure 4 shows experimental and calculated reflectance spectra of s-polarised light incident at angles s-polarised light incident at angles 30° (Figure 4, a) and 60° (Figure 4, b) from RBS of 30 QW GaN/(Al,Ga)N. In all reflectance spectra, the already mentioned Fabry-Perot oscillations are located in the long-wavelength part of the spectrum, which decay as we approach the fundamental absorption edge of the $Al_{0.12}Ga_{0.88}N$ (337 nm). Also in Figure 4, the orange dashed line indicates the exciton resonance wavelength (354 nm).

In Figure 4, a the Bragg peak of reflection from the periodic structure is clearly visible against the background

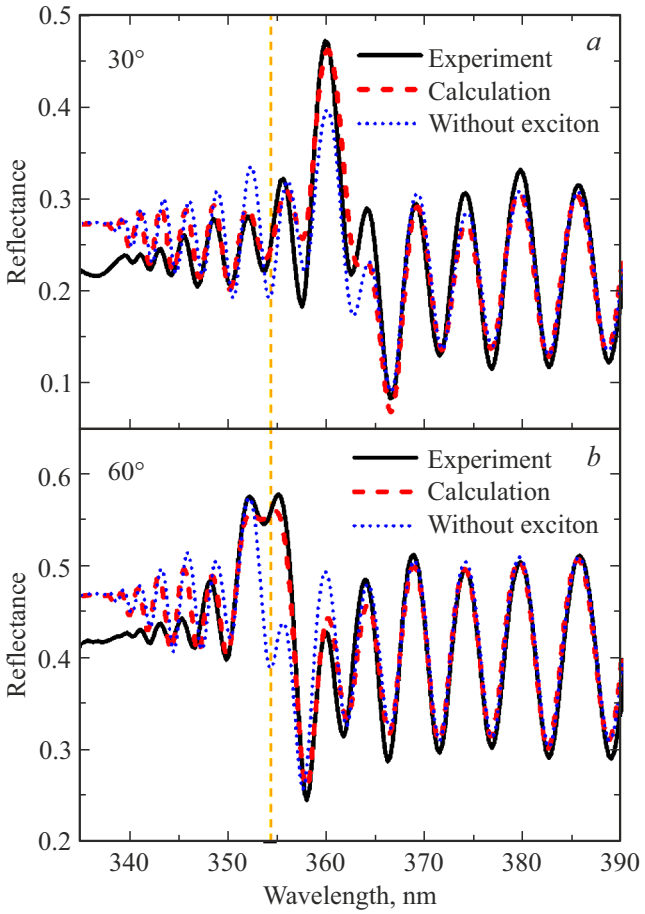

Figure 4. Experimental (solid black lines), calculated with excitons in the QW (dashed red lines), and calculated without considering the exciton contribution (dotted blue lines) spectra of resonant optical reflection from 30 QW GaN/(Al,Ga)N RBS. The light incidence angle is 30 (a) and 60° (b). The exciton resonance wavelength obtained from the calculation is shown by the orange dashed vertical line. Room temperature, s-polarisation of light.

of Fabry-Perot oscillations. The comparison of the experimental reflectance spectrum (solid black line) with the calculated spectrum without the exciton contribution (dotted blue line) shows that the excitons in the QW make a rather weak contribution to the light reflection, since the condition of the double exciton-Bragg resonance is not fulfilled. When the light incidence angle on the RBS increases, the reflection peak shifts to the region of short wavelengths according to the Wolf-Bragg law (Figure 4, b). This incidence angle corresponds to the fulfilment of the Bragg condition near the exciton resonance. In this case, a superradiant exciton-polariton mode is observed in the reflectance spectrum of 30 QW GaN/(Al,Ga)N RBS, the formation of which is accompanied by an increase in the amplitude and half-width of the resonance reflectance band.

In Figure 4, the calculated reflectance spectra taking into account excitons in the QW (dashed red lines) coincide quite closely with the experimental spectra (solid black lines), demonstrating all the key spectral features. The exciton parameters in the calculations are as follows: exciton resonance energy $\hbar\omega_0 = 3.5$ eV, radiative decay parameter $\hbar\Gamma_0 = 0.4 \pm 0.02$ meV, and non-radiative decay parameter $\hbar\Gamma = 40 \pm 5$ meV. The exciton radiative decay $\hbar\Gamma_0$ is a key parameter of the RBS concept and is 0.02–0.03 meV for QW (In,Ga)As/GaAs [12], 0.03–0.04 meV for QW GaAs/(Al,Ga)As [22], 0.04 meV for QW InAs/GaAs [16], 0.05 meV for QW In(As,P)/InP [10], 0.1 meV for QW CdTe/(Cd,Zn)Te [7], 0.2 meV for QW (In,Ga)N/GaN [29,32] and 0.4 meV for QW GaN/(Al,Ga)N [34]. Note that at equal values of non-radiative decay at room temperature, the radiative decay parameter in the GaN QW is 2 times greater than in the GaN/(In,Ga)N QW.

In [54], the authors studied the exciton radiative decay times in the QW when the material of the QW or its surrounding barriers consists of a solid solution with a random distribution of components. It was found that the shortest radiative decay time of a quasi-dimensional exciton is directly proportional to the inhomogeneous broadening of the exciton line in absorption. This leads to the fact that compositional disorder causes a decrease in the Γ_0 parameter. From the comparison of our experimental results for (In,Ga)N/GaN and GaN/(Al,Ga)N QWs, this decrease is ~ 0.2 meV.

The authors of [55] theoretically investigated the effect of inhomogeneous broadening on exciton-light coupling in a single QW and RBS using a semi-classical model. It was assumed that the inhomogeneous broadening of the quasi-dimensional exciton can be described by a Gaussian distribution function. The calculations predict a significant decrease in the radiative width of the RBS superradiant mode when the inhomogeneous broadening is high. These calculations confirm our experimental results for (In,Ga)N/GaN and GaN/(Al,Ga)N QWs.

One can conclude that one of the most important factors lowering the radiative decay of Γ_0 in QW (In,Ga)N is composition fluctuations. This phenomenon is significantly reduced in the case of GaN QWs with (Al,Ga)N barriers. For RBSs with GaN/(Al,Ga)N QWs, we experimentally obtained record high values of the parameter $\hbar\Gamma_0 = 0.4$ meV.

5. Conclusion

In this paper, we present the results of the influence of spatial and energetic disorder on the reflectance spectra of III-N-based RBSs. We have shown that the resonant optical response of RBSs composed of a large number of (In,Ga)N QWs is critically affected by spatial disorder, which can be related to growth rate fluctuations during the growth of thick structures. This is why it is impossible to enhance the resonance properties of RBSs by limitlessly increasing the number of QWs in the system.

A record value of the exciton radiative decay in RBSs from GaN QWs has been obtained compared to other

material systems. The 2-fold increase of the exciton radiative decay in the GaN GaN QW compared to the InGaN QW is due to the decrease of the inhomogeneous broadening of the exciton state. Hence, the development of RBSs made of QWs GaN makes it possible to enhance the resonant optical properties without changing the number of QWs in RBSs.

Conflict of interest

The authors declare that they have no conflict of interest.

References

[1] A. González-Tudela, A. Reiserer, J.J. García-Ripoll, F.J. García-Vidal. Nature Rev. Phys., **6** (3), 166 (2024).
[2] N. Rivera, I. Kaminer. Nature Rev. Phys., **2** (10), 538 (2020).
[3] S. Luo, H. Zhou, L. Zhang, Z. Chen. Appl. Phys. Rev., **10** (1), 011316 (2023).
[4] H.M. Gibbs, G. Khitrova, S.W. Koch. Nature Photonics, **5** (5), 273 (2011).
[5] E.L. Ivchenko, A.I. Nesviszhskii, S. Jorda. Phys. Solid State, **36** (7), 1156 (1994).
[6] E.L. Ivchenko, A.N. Poddubny. Phys. Solid State, **55** (5), 905 (2013). https://doi.org/10.1134/S1063783413050120
[7] Y. Merle d'Aubigne, A. Wasiela, H. Mariette, T. Dietl. Phys. Rev. B, **54** (19), 14003 (1996).
[8] E.L. Ivchenko, V.P. Kochereshko, A.V. Platonov, D.R. Yakovlev, A. Waag, W. Ossau, G. Landwehr. Phys. Solid State, **39** (11), 1852 (1997). https://doi.org/10.1134/1.1130188
[9] J. Sadowski, H. Mariette, A. Wasiela, R. Andre, Y. Merle d'Aubigne, T. Dietl. Phys. Rev. B, **56** (4), R1664 (1997).
[10] W. Yan, X.M. Li, T. Wang. Optics Commun., **285** (24), 4759 (2012).
[11] M. Hübner, J. Kuhl, T. Stroucken, A. Knorr, S.W. Koch, R. Hey, K. Ploog. Phys. Rev. Lett., **76** (22), 4199 (1996).
[12] M. Hübner, J.P. Prineas, C. Ell, P. Brick, E.S. Lee, G. Khitrova, H.M. Gibbs, S.W. Koch. Phys. Rev. Lett., **83** (14), 2841 (1999).
[13] G.R. Hayes, J.L. Staehli, U. Oesterle, B. Deveaud, R.T. Phillips, C. Ciuti. Phys. Rev. Lett., **83** (14), 2837 (1999).
[14] J.P. Prineas, C. Ell, E.S. Lee, G. Khitrova, H.M. Gibbs, S.W. Koch. Phys. Rev. B, **61** (20), 13863 (2000).
[15] J.P. Prineas, C. Cao, M. Yildirim, W. Johnston, M. Reddy. J. Appl. Phys., **100** (6), 063101 (2006).
[16] G. Pozina, M.A. Kaliteevski, E.V. Nikitina, D.V. Denisov, V. Pirogov, L.I. Goray, A.R. Gubaydullin, K.A. Ivanov, N.A. Kaliteevskaya, A.Y. Egorov, S.J. Clark. Sci. Rep., **5**, 14911 (2015).
[17] G. Pozina, K.A. Ivanov, K.M. Morozov, E.I. Girshova, A.Y. Egorov, S.J. Clark, M.A. Kaliteevski. Sci. Rep., **9**, 10162 (2019).
[18] V.V. Chaldyshev, A.S. Shkol'nik, V.P. Evtikhiev, T. Holden. Semiconductors, **40** (12), 1432 (2006). https://doi.org/10.1134/S1063782606120116
[19] V.V. Chaldyshev, A.S. Shkol'nik, V.P. Evtikhiev, T. Holden. Semiconductors, **41** (12), 1434 (2007). https://doi.org/10.1134/S106378260712010X
[20] D. Goldberg, L.I. Deych, A.A. Lisyansky, Z. Shi, V.M. Menon, V. Tokranov, M. Yakimov, S. Oktyabrsky. Nature Photonics, **3** (11), 662 (2009).
[21] V.V. Chaldyshev, Y. Chen, A.N. Poddubny, A.P. Vasilev, Z. Liu. Appl. Phys. Lett., **98** (7), 073112 (2011).
[22] V.V. Chaldyshev, E.V. Kundelev, E.V. Nikitina, A.Yu. Egorov, A.A. Gorbatsevich. Semiconductors, **46** (8), 1016 (2012). https://doi.org/10.1134/S1063782612080052
[23] Y. Chen, N. Maharjan, Z. Liu, M.L. Nakarmi, V.V. Chaldyshev, E.V. Kundelev, A.N. Poddubny, A.P. Vasil'ev, M.A. Yagovkina, N.M. Shakya. J. Appl. Phys., **121** (10), 103101 (2017).
[24] V.V. Chaldyshev, A.S. Bolshakov, E.E. Zavarin, A.V. Sakharov, W.V. Lundin, A.F. Tsatsulnikov, M.A. Yagovkina, T. Kim, Y. Park. Appl. Phys. Lett., **99** (25), 251103 (2011).
[25] A.S. Bolshakov, V.V. Chaldyshev, E.E. Zavarin, A.V. Sakharov, V.V. Lundin, A.F. Tsatsulnikov, M.A. Yagovkina. Phys. Solid State, **55** (9), 1817 (2013). https://doi.org/10.1134/S1063783413090059
[26] V.V. Chaldyshev, A.S. Bolshakov, E.E. Zavarin, A.V. Sakharov, V.V. Lundin, A.F. Tsatsulnikov, M.A. Yagovkina. Semiconductors, **49** (1), 4 (2015). https://doi.org/10.1134/S1063782615010042
[27] A.S. Bolshakov, V.V. Chaldyshev, V.V. Lundin, A.V. Sakharov, A.F. Tsatsulnikov, M.A. Yagovkina, E.E. Zavarin. J. Mater. Res., **30** (5), 603 (2015).
[28] A.S. Bolshakov, V.V. Chaldyshev, E.E. Zavarin, A.V. Sakharov, V.V. Lundin, A.F. Tsatsulnikov. Semiconductors, **50** (11), 1431 (2016). https://doi.org/10.1134/S1063782616110051
[29] A.S. Bolshakov, V.V. Chaldyshev, E.E. Zavarin, A.V. Sakharov, W.V. Lundin, A.F. Tsatsulnikov, M.A. Yagovkina. J. Appl. Phys., **121** (13), 133101 (2017).
[30] S.V. Poltavtsev, I.A. Solovev, I.A. Akimov, V.V. Chaldyshev, W.V. Lundin, A.V. Sakharov, A.F. Tsatsulnikov, D.R. Yakovlev, M. Bayer. Phys. Rev. B, **98** (19), 195315 (2018).
[31] A.A. Ivanov, V.V. Chaldyshev, E.E. Zavarin, A.V. Sakharov, V.V. Lundin, A.F. Tsatsulnikov. Semiconductors, **55** (Suppl. 1), S49 (2021). https://doi.org/10.1134/S1063782621090074
[32] A.A. Ivanov, V.V. Chaldyshev, V.I. Ushanov, E.E. Zavarin, A.V. Sakharov, V.V. Lundin, A.F. Tsatsulnikov. Appl. Phys. Lett., **121** (4), 041101 (2022).
[33] A.A. Ivanov, V.V. Chaldyshev, E.E. Zavarin, A.V. Sakharov, W.V. Lundin, A.F. Tsatsulnikov. Appl. Phys. Lett., **125** (19), 191105 (2024).
[34] A.A. Ivanov, V.V. Chaldyshev, E.E. Zavarin, A.V. Sakharov, W.V. Lundin, A.F. Tsatsulnikov. Appl. Phys. Lett., **123** (12), 121106 (2023).
[35] A. David, C. Weisbuch. Phys. Rev. Res., **4** (4), 043004 (2022).
[36] C. Weisbuch, S. Nakamura, Y.-R. Wu, J.S. Speck. Nanophotonics, **10** (1), 3 (2020).
[37] A. Di Vito, A. Pecchia, A. Di Carlo, M. Auf der Maur. J. Appl. Phys., **128** (4), 041102 (2020).
[38] C.M. Jones, C.-H. Teng, Q. Yan, P.-C. Ku, E. Kioupakis. Appl. Phys. Lett., **111** (11), 113501 (2017).
[39] A. Di Vito, A. Pecchia, A. Di Carlo, M. Auf der Maur. Phys. Rev. Appl., **12** (1), 014055 (2019).
[40] S.Y. Karpov. Photonics Res., **5** (2), A7 (2017).
[41] D.S.P. Tanner, J.M. McMahon, S. Schulz. Phys. Rev. Appl., **10** (3), 034027 (2018).
[42] A. David, N.G. Young, M.D. Craven. Phys. Rev. Appl., **12** (4), 044059 (2019).

[43] D.S.P. Tanner, M.A. Caro, E.P. O'Reilly, S. Schulz. RSC Adv., **6** (69), 64513 (2016).
[44] M. O'Donovan, P. Farrell, J. Moatti, T. Streckenbach, T. Koprucki, S. Schulz. Phys. Rev. Appl., **21** (2), 024052 (2024).
[45] M. Piccardo, C.-K. Li, Y.-R. Wu, J.S. Speck, B. Bonef, R.M. Farrell, M. Filoche, L. Martinelli, J. Peretti, C. Weisbuch. Phys. Rev. B, **95** (14), 144205 (2017).
[46] J. Liu, H. Liang, X. Xia, Q. Abbas, Y. Liu, Y. Luo, Y. Zhang, L. Yan, X. Han, G. Du. J. Alloys Compd., **735**, 1239 (2018).
[47] P. Sohi, J.-F. Carlin, N. Grandjean. Appl. Phys. Lett., **112** (26), 262101 (2018).
[48] M. Auf der Maur, A. Pecchia, G. Penazzi, W. Rodrigues, A. Di Carlo. Phys. Rev. Lett., **116** (2), 027401 (2016).
[49] C.-K. Li, M. Piccardo, L.-S. Lu, S. Mayboroda, L. Martinelli, J. Peretti, J.S. Speck, C. Weisbuch, M. Filoche, Y.-R. Wu. Phys. Rev. B, **95** (14), 144206 (2017).
[50] H.-H. Chen, J.S. Speck, C. Weisbuch, Y.-R. Wu. Appl. Phys. Lett., **113** (15), 153504 (2018).
[51] F. Brunner, V. Hoffmann, A. Knauer, E. Steimetz, T. Schenk, J.-T. Zettler, M. Weyers. J. Cryst. Growth, **298**, 202 (2007).
[52] A. Touré, I. Halidou, Z. Benzarti, T. Boufaden. Microelectronics J., **40** (2), 363 (2009).
[53] S. Schulz, M.A. Caro, C. Coughlan, E.P. O'Reilly. Phys. Rev. B, **91** (3), 035439 (2015).
[54] A.L. Efros, C. Wetzel, J.M. Worlock. Phys. Rev. B, **52** (11), 8384 (1995).
[55] L.C. Andreani, G. Panzarini, A.V. Kavokin, M.R. Vladimirova. Phys. Rev. B, **57** (8), 4670 (1998).

Translated by J.Savelyeva